

SIMULATION OF LIQUID-SOLID FLOW IN A COAL DISTRIBUTOR: INHOMOGENEOUS MODEL VS HOMOGENEOUS MODEL

Baoyu GUO, Kejun DONG and Aibing YU

Lab for Simulation and Modelling of Particulate Systems
School of Materials Science and Engineering
University of New South Wales, Sydney, 2052, Australia

ABSTRACT

Sputnik hydraulic distributor is widely used in a parallel module coal preparation plant. Biased properties in the discharging slurry streams may lead to many problems. To aid the design, control and optimization of the operation, a numerical method has been developed, which consists of a CFD (computational fluid dynamics) model to solve the three-dimensional distribution of water flow and its volume fraction and a DEM (discrete element method) to describe the motion of coal particles in the distributor. Based on this framework, the current paper will present a new set of simulation results using different multi-phase models, i.e., the sophisticated inhomogeneous model and simplified homogeneous model, to simulate water-air flow system in the distributor. Comparison shows apparent differences in the distribution of water volume fraction and velocity. Particularly, the use of the inhomogeneous model gives a clear free water surface in most part of the chamber. The Distribution Performance Index also appears different in pattern. However, in spite of the quantitative differences, the optimal condition identified is consistent in both cases. The effect on the coal particle distribution is further studied by means of CFD-DEM method.

NOMENCLATURE

A	interfacial area
C_D	drag coefficient
\mathbf{F}	force
\mathbf{g}	gravity
I	moment of inertia
m	particle mass
r	volume fraction
p	pressure
\mathbf{T}	torque on particle
t	time
\mathbf{u}	fluid velocity
\mathbf{v}	particle velocity
ρ	density
μ	dynamic viscosity
μ_t	turbulent viscosity
ω	angular velocity of particle
Subscript	
α, β	fluid phase index
i	particle index

INTRODUCTION

Parallel modules are widely applied in coal separation plants in the coal industry due to their good adaptability to

varying productivity, compared with a high capacity unit in a single module. A coal distributor is necessary to split raw coal for subsequent parallel modules. The sputnik hydraulic distributor is widely employed to mix run-of-mine coal and water, and distribute uniformly among a number of outlets to feed the dense medium cyclones in a coal preparation plant. However, industrial sputnik performances deviate considerably from this ideal, and biased properties in the discharging slurry streams often happen.

The flow in a coal distributor involves three phases: coal particles, liquid (water) and air. Experimental studies on the sputnik distributor have been scarce in the literature (Kelly and Holtham, 1996, Holtham and Kelly, 1998, Kelly, 1999). Numerical simulations offer a cost-effective alternative tool to aid the design, control and optimization of the operation. As the carrier fluid of coal particles, the spatial distribution of water flow is essential to the coal distribution. A sputnik coal distributor operating under open conditions contains a large volume of air. Without considering air, the free water surface cannot be simulated by a single fluid model (Rajendran et al., 2006). Although VOF (volume of fluid) method has been employed to track the free surface in a distributor of simple geometry (Yang et al., 1997; Yang, 1999), its application to a complicated condition is extremely difficult, in order to simulate the water distribution in the lower chamber, as in the case being considered currently. Guo et al. (2008) have developed a fully three dimensional CFD model to calculate the water flow. The model performs satisfactorily in that it can predict the key phenomena in a typical sputnik distributor design, as observed on site and in physical experiments. Based on the water flow simulation results, fluid-particle coupling and particle flow behaviours are further investigated by the CFD-DEM method (Dong et al., 2008).

For reasons of computational efficiency and memory requirements for this practical problem, a homogeneous two-phase flow model, which assumes the same velocity for all phases, was used previously to solve the water flow (Guo et al., 2008). Such an assumption, if not valid in all regions of the equipment, must have compromised the predictive accuracy. The current paper will present a new set of simulation results using the more sophisticated inhomogeneous multi-phase model to simulate water-air flow system in the distributor, with a focus on the comparison between these two multiphase models.

MATHEMATICAL MODEL

The flow system in the distributor consists of a number of phases, i.e., water, air and coal particles of different sizes. The CFD-DEM method used here divides the model into two parts and carries out the simulations in parallel. The CFD model is related to the construction of quality finite volume in a complicated geometry and solves the air-water two-phase flow. The DEM part is most suitable for addressing particle-wall and particle-particle interactions. For completeness they are outlined respectively as below.

CFD Model

The commercial CFD software ANSYS-CFX11 (ANSYS Inc., 2007) is used for the water-air flow simulation. The flow is treated as steady and continuous (or Eulerian-Eulerian model), and the Reynolds-averaged mean velocity and other flow quantities are solved. In a general multiphase flow, separate velocity fields and other relevant fields exist for each fluid, so-called "inhomogeneous model".

The continuity equation:

$$\nabla \cdot (r_\alpha \rho_\alpha \mathbf{u}_\alpha) = 0 \quad (1)$$

The momentum equation:

$$\nabla \cdot (r_\alpha \rho_\alpha \mathbf{u}_\alpha \otimes \mathbf{u}_\alpha - r_\alpha (\mu_\alpha + \mu_{t\alpha}) (\nabla \mathbf{u}_\alpha + (\nabla \mathbf{u}_\alpha)^T)) = r_\alpha \rho_\alpha \mathbf{g} - r_\alpha \nabla p + \mathbf{F}_{\alpha\beta} \quad (2)$$

The fluids interact via interphase drag force, calculated as,

$$\mathbf{F}_{\alpha\beta} = \frac{C_D}{8} A_{\alpha\beta} \rho_{\alpha\beta} |\mathbf{u}_\beta - \mathbf{u}_\alpha| (\mathbf{u}_\beta - \mathbf{u}_\alpha) \quad (3)$$

where $\rho_{\alpha\beta} = r_\alpha \rho_\alpha + r_\beta \rho_\beta$, the drag coefficient C_D is set as 0.44 and the interfacial area density is evaluated based on a free surface model,

$$A_{\alpha\beta} = |\nabla r_\alpha| \quad (4)$$

A so-called homogeneous model is a limiting case of a multiphase flow, which assumes the same velocity for all phases but distinct volume fraction, r_α , for each phase α . The fluid flow governing equations are reduced as follows: The continuity equation:

$$\nabla \cdot (r_\alpha \rho_\alpha \mathbf{u}) = 0 \quad (5)$$

The momentum equation:

$$\nabla \cdot (\rho \mathbf{u} \otimes \mathbf{u} - (\mu + \mu_t) (\nabla \mathbf{u} + (\nabla \mathbf{u})^T)) = \rho \mathbf{g} - \nabla p \quad (6)$$

The density, ρ , and laminar viscosity, μ , are valued as the volume fraction weighted average of all the fluid phases considered. Though comparatively more general and computationally cheaper, the homogeneous model, when applied to a distinct free surface flow, is similar to the VOF method, a technique for explicitly tracking a fluid-fluid interface as it changes its topology (Hirt and Nichols, 1981). Their main differences lie in the numerical scheme used to sharpen the volume fraction at the free surface. A Shear Stress Transport turbulence model (SST) is used.

DEM Model

A DEM-based model is used to simulate the particle (coal) motion in the distributor. According to this method, the translational and angular motion of each coal particle is described by the following equations:

$$m_i \frac{d\mathbf{v}_i}{dt} = \mathbf{F}_i \quad (7)$$

$$I_i \frac{d\boldsymbol{\omega}_i}{dt} = \mathbf{T}_i \quad (8)$$

where \mathbf{F}_i is the sum of all the forces acting on particle i , including the contact forces, the gravity and also the fluid-particle interaction forces (Xu et al., 2000).

Limited by the current computational abilities, the one-way coupling method was used in this work, where only the fluid-particle interactions on the coal particles are considered in the DEM simulation, whereas the effect of coal particles on the fluid flow is ignored.

GEOMETRY AND MODELING CONDITION

This work is focused on the examination of different models to describe gas-liquid flow. For the purpose of comparison, the geometry used is the same as used in the previous studies (Guo et al., 2008). Figure 1 shows the geometric configuration and coordinates used and Figure 2 shows the layout of water inlet nozzles and outlet numbering. Two chambers are separated by a horizontal orifice plate in the middle; a disk splitter is placed in the upper chamber to direct the charged slurry on to the orifice plate. Eight slots are open on the orifice plate. All eight tangential water inlets are intruded into the cylinder respectively at two levels with a tip bevel angle of 45 degree. Outlet diameter is 145 mm.

The top charging port is set as a uniform water inlet. An inlet boundary is set on the bevel face at the tip of each intruding tube for the tangential water entry tube so that the flow inside each tube is not considered. Uniform velocity is aligned with the axial direction of the tube.

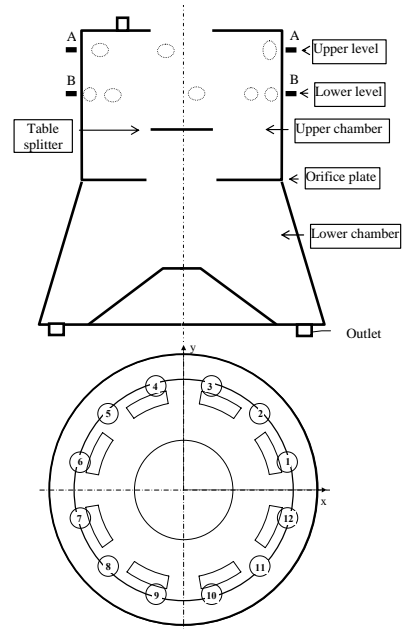


Figure 1: Schematic illustration of the distributor considered: side and plan view of geometry, internal structure and numbering of outlets.

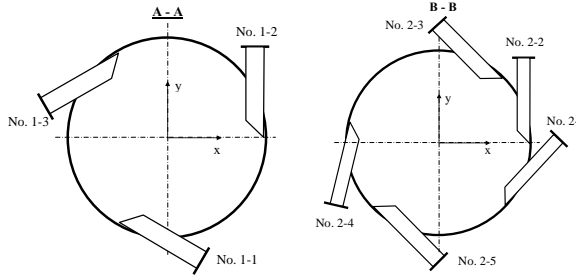


Figure 2: Orientation and numbering of inlets.

Table 1 lists the water condition in the existing operation and for all the cases considered. The water flowrate varies widely among the tangential inlets, ranging 0 - 1000 m³/hr under the existing operation conditions. This led to a strongly biased tangential momentum over the circumference, so it was not surprising that the slurry stream was unevenly split among these outlets. Based on the existing pipe layout, we chose three cases as the potential modifications where the operating water flowrates through each tangential inlet are adjusted without changing the total water consumption. The three cases are featured respectively by evenly spaced three inlets of 250mm (C1), two evenly spaced inlets of 250mm (C2), and two nearly evenly spaced inlets of 200mm (C3).

Table 1: Water inlet conditions for different cases

Inlet No.	Position	Diameter (mm)	Water flowrate (m ³ /hr)			
			Existing	C1	C2	C3
1-1	Upper level	250	0	567	0	0
1-2		250	0	567	0	0
1-3		250	1000	567	0	0
2-1	Lower level	200	117	0	0	0
2-2		200	117	0	0	850
2-3		250	233	0	850	0
2-4		200	0	0	0	850
2-5		250	233		850	0
Top		1150	400	400	400	400
Total			2100	2100	2100	2100

RESULTS AND DISCUSSION

The simulations are carried out on the fixed mesh with total number of grid points of one million. An “iso-volume”, defined as the region with water volume fraction above 0.5, is used to graphically display the three-dimensional pattern of water distribution. For quantitative analysis, an Distribution Performance Index is defined as

$$DPI = \frac{M_{outlet}}{\sum M_{outlet}} \times n, \text{ where } M_{outlet} \text{ is the mass flowrate of}$$

water or coal particles from each outlet, and n is the total number of outlets. Its standard deviation

$$SD = \sqrt{\frac{1}{n} \sum (DPI - 1)^2} \text{ indicates the overall}$$

performance.

It is well known that the choice of the inhomogeneous model requires a larger computer memory and longer CPU time than the simpler homogeneous model. The simulation results using both models will be compared. For convenience, the inhomogeneous model and the homogeneous model are referred to as Model-A and Model-B respectively.

Typical Results

Firstly the general features of the simulation results, taking Case C3 as an example, are described. As shown by the iso-surface in Figure 3 and Figure 4, air fills most of the space in the upper chamber, and the water distribution is rather non-uniform. The water stream from the coal charging port at the top falls directly on the table splitter and is then directed towards the orifice plate. Water jets exiting the water inlets impact on the cylindrical surface, and then flow along the surface in a downward spiral. The jets spread gradually in terms of the contact area with the cylinder. The spiral pattern is extended all the way down to the lower chamber through the open slots. Swirling is seen to exist in both the upper chamber and the lower chamber. Centrifugal force causes a certain amount of water to build up at the corner above the orifice plate, while a concave water surface shape is generated in the lower chamber. A smaller overflow through the central orifice is also observed.

Qualitative comparison

The modelling results show apparent differences between the two models in terms of the distribution of water volume fraction and velocity. Figure 4 visualizes the free surface. Figure 5 is the water volume fraction in a plane passing the centre axis. Particularly, the use of Model-A gives a sharp free water surface in the lower chamber as well as above the orifice plate. In the lower chamber, the water surface looks relatively flat, with some irregular pits and humps generated by the impact of the falling streams from the slots. When using Model-B, on the other hand, the air-water boundary is not clear-cut in the lower chamber, i.e., a volume fraction of zero or one can not be achieved on each side of the free surface. The free surface shows a more curved but regular shape, so that the water level at the centre is much lower than the surrounding region. Moreover, Model-B predicts a contracting stream falling from the top port down to the table splitter, while Model-A always predicts dispersed water distribution and an accumulated layer on the table splitter.

The superficial velocity vectors (Figure 6) show that, although there is a relatively high velocity near the side wall for both models, the overall velocity fields are very different above/below the table splitter. Moreover, Model-A predicts a higher velocity at the water surface, while Model-B predicts a relatively uniform velocity distribution in most part of the equipment except in the top stream zone above the table splitter.

The predicted DPIs by both models are compared in Figure 7. For Case C3, the optimal condition with smallest SD value, similar, relatively uniform patterns are produced by both models, although the exact locations of the minimum and maximum may slightly differ. However, for other cases, the DPIs may become more different. For C2, although both models predict a similar cyclic pattern with double peaks, the peak locations are 90 degree apart.

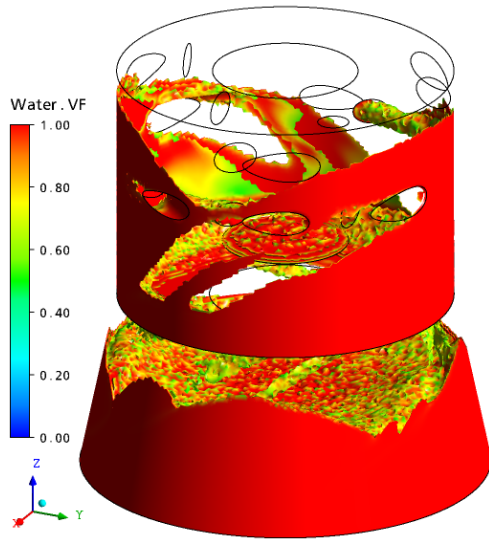
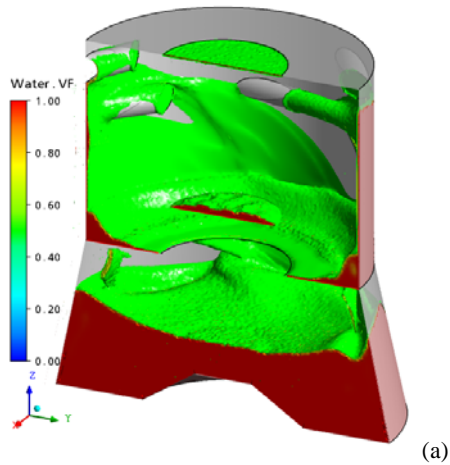
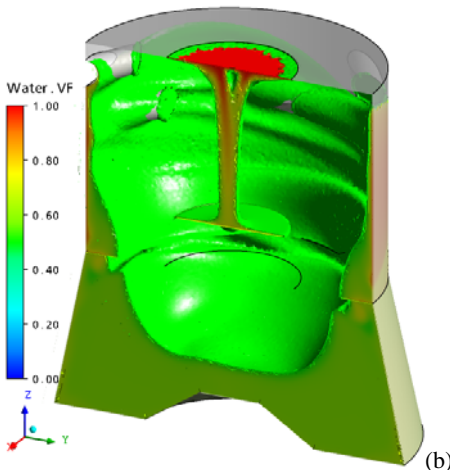


Figure 3: Iso-surface of water volume fraction showing the flow pattern for the case of C3 using Model-A.

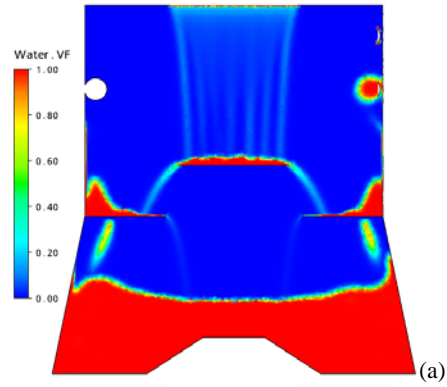


(a)

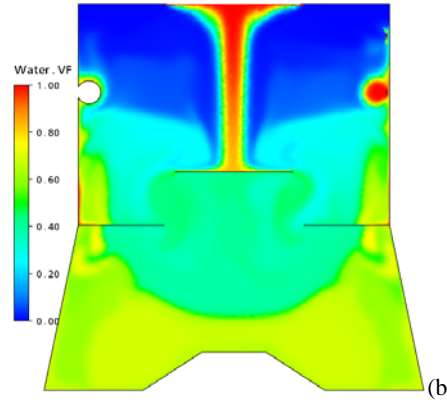


(b)

Figure 4: Clipped iso-surface of water volume fraction for Case C3. (a) Model-A; (b) Model-B.

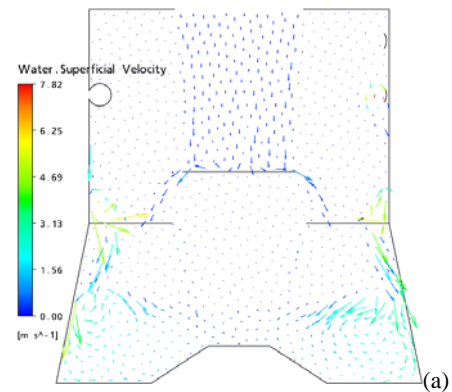


(a)

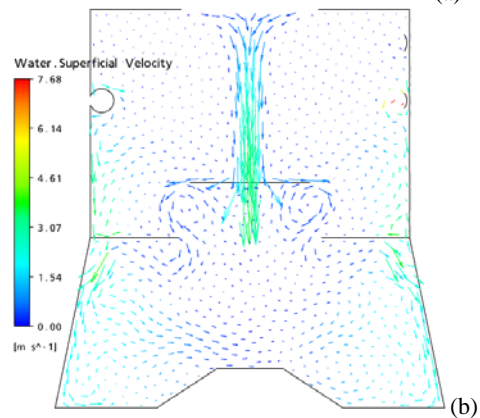


(b)

Figure 5: Water VF isopleths for Case C3 on X-Z plane. (a) Model-A; (b) Model-B.



(a)



(b)

Figure 6: Superficial velocity vectors of water for Case C3 on X-Z plane; (a) for Model-A; (b) for Model-B.

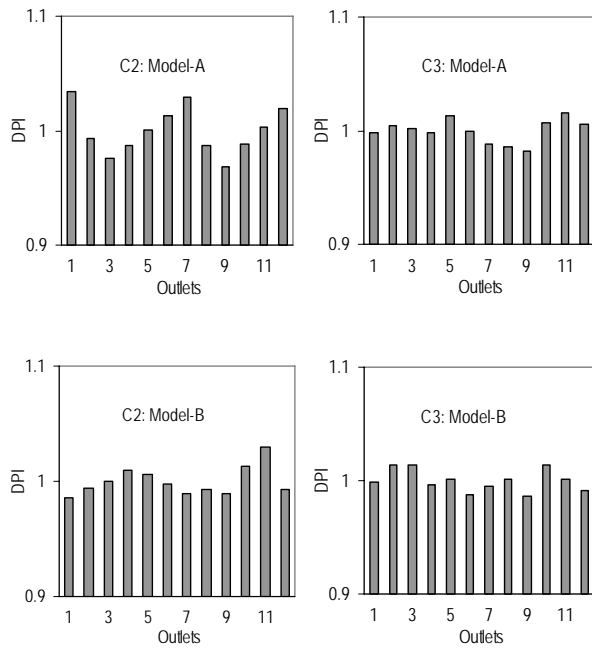


Figure 7: Comparison of DPIs for Cases C2 and C3

Quantitative Comparison

Table 2 lists the predicted SD values for DPIs and some other quantities that would also affect the interaction with the particles. The water holdup should affect the ability to suspend the particles, and the total tangential momentum reflects the driving force to mix particles in the tangential direction.

Although the water holdup and total momentum predicted by both models are very close in the lower chamber, their differences are significant in the upper chamber. For example, Model-B has predicted a much higher holdup in the upper chamber than Model-A by 3-5 times.

Comparison of the SD values indicates: (a) Model-A tends to predict a slightly greater SD value; (b) Model-A and Model-B predict a consistent trend for operational optimization in terms of the overall uniformity of the outflows. Such an agreement, if not a fortuitous coincidence, is probably due to the similar trend in the total water momentum in both chambers. Among the three cases considered, C3 provides an optimal condition for uniform outflow distribution (with minimum SD value), whereas C2 causes the worst outflow distribution. Literally, a large number of evenly spaced inlets and high water inlet momentum should favour the uniformity of the outflows. In Case C3, fewer and yet biased locations of the inlets would adversely affect the DPI. However, their smaller diameters lead to a stronger tangential momentum that is sufficient to compensate for the adverse effect. Therefore, Case C3 performs relatively better than the other cases.

Table 2: A list of water flow quantities predicted

Quantity	Model	Case		
		C1	C2	C3
Total tangential momentum in upper chamber, kg m s^{-1}	A	629	1177	2008
	B	2422	2664	3480
Total tangential momentum in lower chamber, kg m s^{-1}	A	6624	9660	11650
	B	7361	9627	12381
Total water holdup in upper chamber, m^3	A	0.775	0.823	0.904
	B	3.702	2.765	2.785
Water holdup in lower chamber, m^3	A	5.622	5.471	5.592
	B	5.263	5.536	5.607
SD of DPI	A	1.44%	2.07%	0.99%
	B	1.13%	1.21%	0.91%

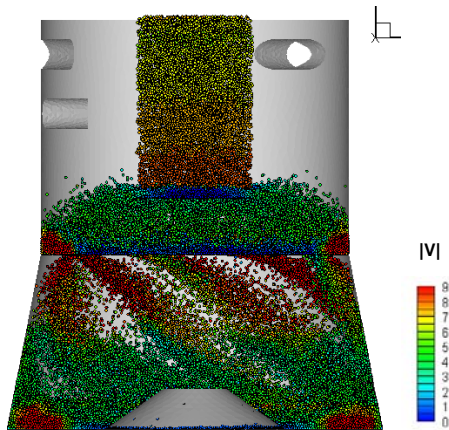
Particle Flow

The coal particles are represented by spheres with 20mm in diameter. The charging rate is 1500 t/hr. Figure 8 shows a snapshot of particles in a side view. Despite the differences in the water flow field, due to use of Model-A or Model-B, the overall particle flow patterns predicted look very similar. Generally, in the upper chamber, particles fall down uniformly from the charging port, and hit the table splitter. Then they are bounced on to the orifice plate and spread out widely. Several streams are formed, most of which run through the different open slots, and the rest fall down from the central orifice. Finally they fall on the bottom surface of the distributor and keep swirling with water flow until flowing out through one of the outlet holes.

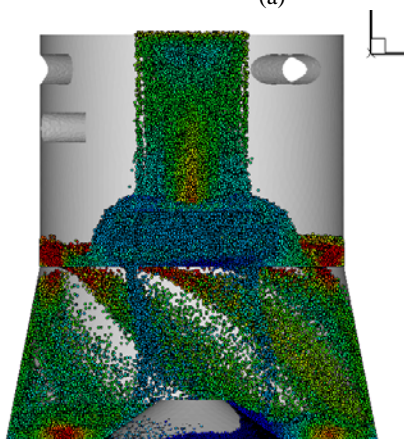
Different water flow fields do result in some noticeable differences in the particle flow in some regions, particularly in the upper chamber: (a) When using Model-A, particles, after hitting the table splitter, are more easily carried outward in the radial direction, so that they appear splashier. (b) When using Model-B, a relatively larger proportion of particles fall down through the central orifice.

The DPI distribution of particle flow is generally much worse than that of water flow, but a roughly corresponding relationship exists for SD of DPI between water flow and particle flow for most of the cases considered (Figure 9). The particle distribution tends to improve as water flow distribution improves. Therefore, an optimal water condition should provide an optimal particle flow distribution.

In views of these differences discussed above, the results predicted using the inhomogeneous model seem to make more sense physically. In this case, separate velocities for different phases allow phase-phase interaction and inter-penetration; therefore the water may disperse and settle down easily depending on the total forces applied.



(a)



(b)

Figure 8: A snapshot of particle flow for Case C3. (a) Model-A; (b) Model-B. (color scaled to velocity).

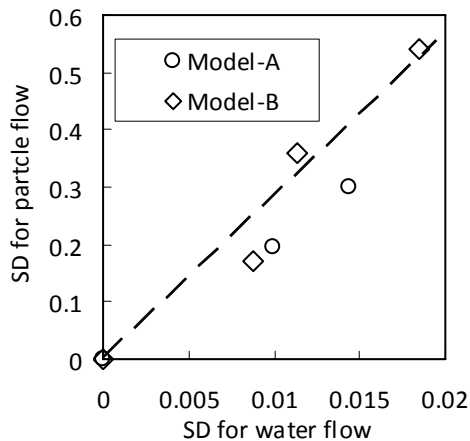


Figure 9: SD of DPI: particle flow versus water flow.

CONCLUSION

This paper has compared the two multiphase models, i.e., inhomogeneous model and homogeneous model, when applied to the simulation of the water-particle flow in a coal distributor. Different models have predicted apparently different distribution in water volume fraction and velocity. Particularly, the use of the inhomogeneous model gives a clear free water surface in most of the chamber and significantly smaller water holdup/

momentum in the upper chamber. The inhomogeneous model generates more physically meaningful predictions and should be used preferentially over the homogeneous model. Both models give a consistent trend in the standard deviation of DPI for different water inlet conditions. Finally, CFD-DEM simulation results show that the choice of different multiphase models makes some differences in the particle flow distribution, but the optimal water flow condition identified applies to the particle flow.

ACKNOWLEDGEMENT

Useful discussions at the initial stage of the work with A. Vince (currently in Elsa Consulting Group Pty Ltd) and I. Brake (BHP Billiton Mitsubishi Alliance) are gratefully appreciated.

REFERENCES

- ANSYS Inc., (2007), ANSYS CFX-11.0-user online manual.
- DONG, K.J., GUO, B.Y., CHU, K.W., YU, A.B. and BRAKE, I., (2008), "Simulation of liquid-solid flow in a coal distributor", *Minerals Engineering*, **21**, 789-796.
- GUO, B.Y., DONG, K.J., CHU, K.W. YU, A.B., VINCE, A. and BRAKE, I., (2009), "A numerical model for the liquid flow in a sputnik coal distributor", *Minerals Engineering*, **22**, 78-87.
- HIRT, C.W. and NICHOLS, B.D., (1981), "Volume of fluid (VOF) method for the dynamics of free boundaries", *J. Com. Physics*, **39**, 201-225.
- HOLTHAM, P. and KELLY, R., (1998), Control of Hydraulic Distributors to Minimize Feed Bias to Plant Modules, ACARP Project C4055, report.
- KELLY, R. and HOLTHAM, P., (1996), "An investigation of industrial raw coal distributor, part A experiment", *Proc. 24th Australian & New Zealand Chem. Eng. Conf.*, Chemica'96, Vol.3, : Institution of Engineers, Australia, Barton, A.C.T., 23-28.
- KELLY, R., (1999), Model and Industrial Investigation of the Sputnik Raw Coal Distributor, PhD thesis, University of Queensland.
- RAJENDRAN, S. NARASIMHA, M., DUTTA, A., SINHA, M. K. and MISRA, A., (2006), "Modelling of feed distributor at coal washeries", *Int. J. Miner. Process.*, **81**, 178-186.
- XU, B.H., YU, A.B., CHEW, S.J. and ZULLI, P., (2000), "Numerical simulation of the gas-solid flow in a bed with lateral gas blasting", *Powder Technology*, **109**, 13-26.
- YANG, D., (1999), Computational Modelling for Coal Slurry Distributor Flow, PhD thesis, University of New South Wales, 1999.
- YANG, D., FLETCHER, C. A. J. and PARTRIDGE, A. C., (1997), "Computational modelling of coal slurry distributor flows", *Proc. 1st Int. Conf. on CFD in Mineral & Metal Processing and Power Generation*, Melbourne, Australia, 125-132, 1997.